JOURNAL OF THERMOPHYSICS AND HEAT TRANSFER
Vol. 21, No. 1, January–March 2007

State-Resolved Dissociation Rates for Extremely Nonequilibrium Atmospheric Entries

M. Lino da Silva,* V. Guerra,† and J. Loureiro†
Instituto Superior Técnico, 1049-001 Lisboa, Portugal

DOI: 10.2514/1.24114

This paper presents the application of the forced harmonic oscillator method to the simulation of state-resolved dissociation processes behind high-temperature shock waves typical of atmospheric reentries. Improvements have been brought to the model, considering a more precise method for the calculation of the different vibrational level energies, therefore increasing the accuracy of the predicted transition probabilities between higher vibrational levels close and above the dissociation limit. The model has been validated against data issued from recent experiments, as well as data issued from semiclassical trajectory calculations for collisions between different species. A good overall agreement is achieved against such other data. A database of reaction rates has been constructed with the purpose of simulating shock-heated nitrogen flows. Dissociation processes behind a shock wave have been simulated for different postshock translational temperatures. At lower temperatures, the well-known ladder-climbing phenomenon is the main dissociation channel behind a shock wave, with dissociation occurring for transitions from the vibrational levels close to the dissociation limit. At higher temperatures, transitions between the different vibrational levels of nitrogen become roughly equiprobable, and the overall range of bound vibrational levels contributes to the dissociation.

Nomenclature

C_{ij}^k	=	transformation matrix
C_p	=	specific heat at constant pressure, J/kg/K
C_v	=	specific heat at constant volume, J/kg/K
E	=	level energy, Hz
E_m	=	Morse potential well, J
h	=	enthalpy, J/kg
J_s	=	Bessel function
k_B	=	Boltzmann constant, $1.3806505 \times 10^{-23}$ J/K
$k(T)$	=	thermal reaction rate, cm^3/s
M	=	Mach number
m	=	mass, kg
$\tilde{m}$	=	mass parameter, $m_{AB}m_C/(m_{AB}+m_C)$ or $m_{AB}m_{CD}/(m_{AB}+m_{CD})$
P	=	probability
r	=	internuclear distance, m
S_{VT}	=	vibration-translation steric factor, 4/9
S_{VV}	=	vibration-vibration steric factor, 1/27
T	=	macroscopic temperature, K
T_r	=	rotational temperature, K
T_{tr}	=	translational temperature, K
$T_{\mathrm{tr-r}}$	=	translational-rotational temperature, K
T_v	=	vibrational temperature, K
t	=	time, s
$V(r)$	=	intermolecular potential, J
V-T	=	vibration-translation processes
V-V-T	=	vibration-vibration-translation processes
v	=	vibrational level
v	=	velocity, m/s
$\bar{v}$	=	averaged collision velocity, m/s
Z	=	gas-kinetic collisional frequency, Hz
α	=	repulsive potential parameter, m^{-1}
γ	=	heat capacity ration, C_p/C_v
γ	=	mass parameter, $m_A/(m_A+m_B)$
ε	=	two-state first-order V-T transition probability, $P(1 \rightarrow 0)$
μ	=	mass parameter, $m_A m_B/(m_A+m_B)$
ρ	=	two-state first-order V-V-T transition probability, $[4P(1,0 \rightarrow 0,1)]^{1/2}$
ρ_ξ	=	generalized two-state first-order V-V-T transition probability
σ	=	collision cross section, m^2
ω	=	vibrational transition frequency, Hz
ω_e	=	harmonic oscillator energy, Hz
$\omega_e x_e$	=	first-order anharmonic oscillator energy, Hz

Subscripts

f	=	final vibrational quantum number
i	=	initial vibrational quantum number
max	=	maximum vibrational level before dissociation
qbound	=	vibrational level above the dissociation limit
tr	=	translational mode
vib	=	vibrational mode
0	=	preshock
1	=	postshock

I. Introduction

SPECIAL focus is currently being brought to high-temperature kinetic phenomena behind high-speed shock-waves. Advances in the qualitative and quantitative understanding of such postshock phenomena [1–4] are being driven by the definition of interplanetary missions involving the entry (or reentry) of a spacecraft in a planetary atmosphere. Maneuvers such as planetary aerobraking, aerocapture, or direct entry of a spacecraft inbound from another planet follow hyperbolic trajectories where crossing of the planetary atmosphere occurs at velocities well in excess of 10 km/s. For example, a direct entry in Earth atmosphere from planet Mars occurs at 11 km/s ($M = 44$). Comparatively, a Space Shuttle entry from Earth's orbit occurs at most at 7 km/s ($M = 28$) [5].

The well-known Rankine–Hugoniot shock relations allow the determination of the postshock translational temperature T_1 according to the equation

Received 22 March 2006; revision received 17 May 2006; accepted for publication 18 May 2006.

*Researcher, Centro de Física dos Plasmas, Av. Rovisco Pais; mlinodasilva@mail.ist.utl.pt. Member AIAA.

†Professor, Centro de Física dos Plasmas, Av. Rovisco Pais.

$$\frac{T_1}{T_0} = \frac{[2\gamma M^2 - (\gamma - 1)][2 + (\gamma - 1)M^2]}{(\gamma + 1)^2 M} \quad (1)$$

with T_0 denoting the preshock temperature and $\gamma = C_p/C_v$.

In diatomic gases, some relaxation to the rotational and vibrational modes is immediately established behind the shock wave, lowering the translational temperature. However, if the shock wave is considered as a discontinuity (continuum flow regime), the translational temperature obtained immediately behind the shock wave corresponds to the value determined using Eq. (1). In the hypersonic limit, all the translational energy of the flow can be considered to be converted to its internal modes: the coherent kinetic energy of the flow particles is firstly transferred to the thermal agitation mode defined by the translational temperature for a Maxwellian velocity distribution function of the particles, and latterly to the rotational and vibrational modes of the diatomic molecules, defined by the temperatures T_r and T_v, respectively, for a Boltzmann distribution of such levels populations. In such limiting case, the calculation of the postshock translational temperature proceeds very simply:

$$\frac{1}{2}mv_0^2 = \frac{5}{2}k_B(T_{\text{tr}})_1 + ak_B(T_{\text{tr-r}})_1 \Leftrightarrow (T_{\text{tr}})_1 = \frac{mv_0^2}{(5 + 2a)k_B} \quad (2)$$

where a is a constant set to 1 if instantaneous equilibration of the rotational temperature $(T_r)_1$ with the translational temperature $(T_{\text{tr}})_1$ is considered, and 0 if the rotational temperature $(T_r)_1$ is considered to remain at its preshock value $(T_r)_0 = (T_{\text{tr}})_0$.

It is easy to conclude that the understanding of the physical-chemical processes behind hyperbolic shock waves requires the development of theoretical models valid at very high translational temperatures. Applying Eq. (2) (with $a = 1$) to the aforementioned entry flight speeds, one obtains a postshock translational temperature of 60,000 K for a direct entry from planet Mars, and a translational temperature of 24,000 K for a Shuttle entry from orbit. In brief, the development of physical-chemical models valid at such temperatures acquires a particular relevance in the scope of programs such as the ESA-sponsored AURORA program for the exploration of the solar system.

For all practical purposes, equilibration of the translational and rotational modes of the flow molecules can be usually considered as instantaneous behind a shock wave. Excitation of the molecular vibrational modes (V-T processes) occurs more slowly, and in very strong nonequilibrium (non-Boltzmann) conditions. Dissociation reactions follow the excitation of the molecular vibrational modes, and are latterly followed by ionization reactions which bring the flow to a plasma state where electron-impact processes become dominant [6].

An adequate description of such excitation processes requires the definition of the so-called state-to-state models, where a description of the energy exchanges between the different vibrational levels of the flow molecules and their translational energy is developed.

Previous works on this issue have typically resorted to simpler approaches derived from other fields such as gas discharges [7–9]. It is not until recently that it has been acknowledged that the specific conditions encountered behind strong shock waves required developing and using more elaborate theoretical approaches [10,11].

This work presents the development of a state-to-state model for the description of the vibrational excitation and dissociation processes behind very high-speed shock waves. A numerical model has been developed according to the requirements aforementioned (validity at very high translational temperatures), and has been validated against experimental and other models' data. Care has been exerted in using the most precise data for the description of the different molecular energy levels and their interactions, while retaining an affordable computational cost. A database of rate coefficients has been obtained for the simulation of postshock nitrogen flows (the major species encountered in Earth's atmosphere entry flows), and is discussed in order to check the validity of the model and the different assumptions applied in our work. The different channels through which dissociation proceeds behind a shock wave are also investigated for several limiting cases.

II. Theoretical Models for the Prediction of V-T and V-V-T Rates

Populations of the molecular vibrational levels are controlled by vibration-translation processes in diatom-atom collisions:

$$AB(i) + C \rightleftarrows AB(f) + C \quad (3)$$

and by vibration-vibration-translation processes in diatom-diatom collisions:

$$AB(i_1) + CD(i_2) \rightleftarrows AB(f_1) + CD(f_2) \quad (4)$$

where i and f represent the initial and final vibrational quantum numbers for the AB molecule (index 1) and the CD molecule (index 2).

A. Basic Trends of the Models

The first-order approach for the simulation of such processes is the semiclassical first-order perturbation theory (FOPT). Namely, a collinear collision model taking into account a repulsive intermolecular potential is given by the Schwartz, Slawsky, and Herzfeld (SSH) theory [12,13] and its extensions [14–20]. This theory is capable to simulate single-jump transition probabilities in conditions where these are much smaller than unity. This is the case for the simulation of state-to-state processes in gas discharges where this theory can be successfully applied [21].

For high-energy flows, where high collision velocities are attained, V-T and V-V-T transition probabilities, including multiquantum transitions, become large, preventing them from being correctly predicted by FOPT models. Moreover, at high collision velocities, FOPT models predict unphysical transition probabilities larger than unity for the higher vth levels [22,23].

More precise models include exact quantum models [24–27] and semiclassical models such as the ones developed by Billing [22] and applied to the simulation of molecular collisions [28–33]. Such models allow the calculation of more accurate transition probabilities than FOPT models but require a large amount of computer resources (namely for full quantum calculations), making them unpractical for the systematic calculation of transition probabilities in diatomic gases.

Finally a semiclassical nonperturbative analytic method exists which allows the calculation of V-T and V-V-T transition probabilities for a harmonic oscillator acted upon by an external exponential force [34–36]. This method is called the forced harmonic oscillator (FHO) and provides a semiclassical nonperturbative analytical solution for V-T and V-V-T transition probabilities, which compares well with exact quantum methods and the quantum-classical trajectory (QCT) method developed by Billing [22]. More recently, Adamovich et al. have successfully applied this method to the simulation of postshock flows, and extended its scope of application to include 3-D collision trajectories and molecular rotation effects [10,23,37–41].

B. Overline of the FHO Model

This section summarizes the main expressions for the calculation of V-T and V-V-T transition probabilities in collinear atomic-diatomic and diatomic-diatomic collisions.

V-T transition probabilities for collinear atom-diatom nonreactive collisions are given by Kerner [34] and Treanor [35]

$$P(i \to f, \varepsilon) = i!f!\varepsilon^{i+f}\exp(-\varepsilon)\left|\sum_{r=0}^{n}\frac{(-1)^r}{r!(i-r)!(f-r)!\varepsilon^r}\right|^2 \quad (5)$$

with $n = \min(i, f)$.

V-V-T transition probabilities for collinear diatom-diatom collisions are given[‡] by Zelechow et al. [36]

[‡]Corrected from typographic errors

$$P(i_1, i_2 \to f_1, f_2, \varepsilon, \rho) = \left| \sum_{g=1}^{n} (-1)^{(i_{12}-g+1)} C_{g,i_2+1}^{i_{12}} C_{g,f_2+1}^{f_{12}} \times \varepsilon^{\frac{1}{2}(i_{12}+f_{12}-2g+2)} \exp(-\varepsilon/2) \sqrt{(i_{12}-g+1)!(f_{12}-g+1)!} \times \exp[-i(f_{12}-g+1)\rho] \times \sum_{l=0}^{n-g} \frac{(-1)^l}{(i_{12}-g+1-l)!(f_{12}-g+1-l)!l!\varepsilon^l} \right|^2 \quad (6)$$

with $i_{12} = i_1 + i_2$, $f_{12} = f_1 + f_2$, and $n = \min(i_1 + i_2 + 1, f_1 + f_2 + 1)$.

In these equations ε and ρ are related to the two-state FOPT transition probabilities, with $\varepsilon = P_{\text{FOPT}}(1 \to 0)$ and $\rho = [4P_{\text{FOPT}}(1, 0 \to 0, 1)]^{1/2}$. Finally, C_{ij}^k is a transformation matrix calculated according to the expression[§]

$$C_{ij}^k = 2^{-n/2} \binom{k}{i-1}^{-1/2} \binom{k}{j-1}^{1/2} \sum_{v=0}^{j-1} (-1)^v \binom{k-i+1}{j-v-1} \binom{i-1}{v} \quad (7)$$

For a purely repulsive intermolecular potential $V(r) \sim \exp(-\alpha r)$, expressions for ε and ρ are given by Zelechow et al. [36]

$$\varepsilon = \frac{8\pi^3 \omega (\tilde{m}^2/\mu)\gamma^2}{\alpha^2 h} \sinh^{-2}\left(\frac{\pi\omega}{\alpha\bar{v}}\right) \quad (8)$$

$$\rho = 2(\tilde{m}^2/\mu)\gamma^2 \alpha \bar{v}/\omega \quad (9)$$

whereas for a Morse intermolecular potential $V(r) \sim E_m[1 - \exp(-\alpha r)]^2$, the expression for ε is given by Cottrell and Ream [19]

$$\varepsilon = \frac{8\pi^3 \omega (\tilde{m}^2/\mu)\gamma^2}{\alpha^2 h} \frac{\cosh^2\{[(1+\phi)\pi\omega]/\alpha\bar{v}\}}{\sinh^2(2\pi\omega/\alpha\bar{v})} \qquad \phi = (2/\pi)\tan^{-1}\sqrt{(2E_m/\tilde{m}\bar{v}^2)} \quad (10)$$

with an expression for ρ identical to Eq. (9). Here E_m represents the potential well, ω denotes the oscillator frequency, and μ, γ, and $\tilde{m}$ are mass parameters [23,38].

C. Improvements to the FHO Model

To allow a successful application of the FHO model to the prediction of transition probabilities, several improvements need to be brought to the aforementioned expressions. These have previously been discussed by Adamovich et al. [23,38], and they have been considered during the development of our model. In short, these include the following:

1) Symmetrization of the collision velocity to enforce detailed balance (a median collision velocity $\bar{v} = (v_i + v_f)/2$ is considered).

2) Accounting for the anharmonicity of the oscillator potential curve using an average frequency $\omega = |(E_i - E_f)/(i - f)|$ if $i \neq f$, and $\omega = |E_{i+1} - E_i|$ if $i = f$.

3) Generalization of the model for nonresonant V-V-T transitions and V-V-T transitions between different species, by replacing $\rho \to \rho\xi/\sinh(\xi)$, with $\xi = \pi^2(\omega_1 - \omega_2)/4\alpha\bar{v}$

4) Generalization of the FHO model to noncollinear collisions (general case) through the multiplication of the parameters ε and ρ by steric factors such that $\varepsilon = \varepsilon S_{\text{VT}}$ and $\rho = \rho\sqrt{S_{\text{VV}}}$, using the values $S_{\text{VT}} = 4/9$ and $S_{\text{VV}} = 1/27$, as proposed by Adamovich et al. [23,38].

An additional improvement to the model is proposed in this paper, concerning the calculation of the energies of vibrational levels which are usually carried according a polynomial expansion of the type

[§]Also corrected from typographic errors

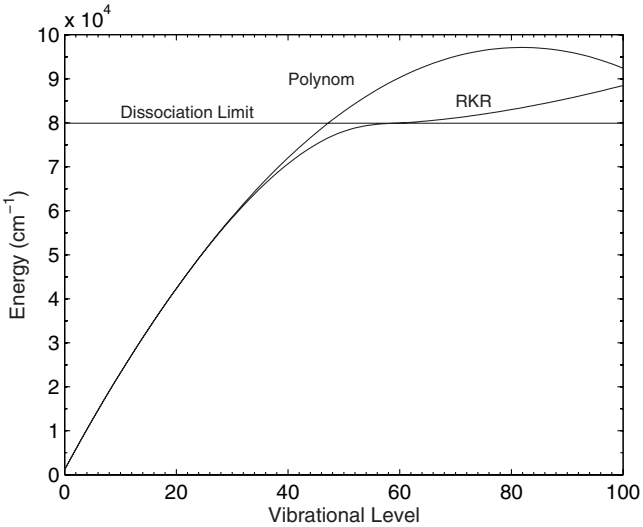

Fig. 1 Calculated vibrational level energies for the ground state of N_2.

$$E_{i,f} = \omega_e\left(v + \frac{1}{2}\right) - \omega_e x_e\left(v + \frac{1}{2}\right)^2 \quad (11)$$

where ω_e and $\omega_e x_e$ are spectroscopic constants obtained in the literature for different molecular electronic levels.

It is well known that this expression cannot be accurately applied to the calculation of vibrational level energies close and above the dissociation limit. Therefore, a more accurate calculation of the vibrational level energies is carried through the reconstruction of potential curves according to the Rydberg–Klynning–Rees (RKR) method, and the resolution of the radial Schrödinger equation for this potential curve, as described in another work [42]. The predicted maximum vibrational level of N_2 corresponds in this case to $v_{\max} = 59$ instead of $v_{\max} = 45$ predicted when the polynomial expansion of Eq. (11) is used. Figure 1 depicts the differences between the vibrational levels energies calculated using polynomial expansions or the RKR method. Differences in the levels' energies become apparent for $v > 30$. As it will be discussed more in following sections, the application of this method has a considerable impact on the prediction of the V-T and V-V-T rates through the FHO model.

D. Scope and Validation of the FHO Model

The FHO model described in this paper, remaining based on a simplified collision model, cannot be straightforwardly applied to the simulation of any collisonal process. As the model does not account for molecular rotational motion, it cannot be directly applied to molecules with low reduced masses such as hydrogen molecules, in which vibration-rotation effects are important. Also, the model cannot predict reactive collisions or collisions involving non-adiabatic electronic transitions, such as NO-NO collisions. Also, multipole-multipole attractive forces (only important at lower temperatures) are not considered here, but could be included through the collision parameters ε and ρ, calculated according to a Lennard–Jones potential [38].

Experimental measurements of state-to-state rate coefficients remain scarce and limited to low temperatures and lower quantum numbers [43–47]. The validation of the FHO method has therefore to be carried against very precise models of molecular collisions. Among these, the results from the QCT method developed by Billing, and applied to the description of N_2-N_2 [29], N_2-N [48,49], N_2-O_2 [31], and O_2-O_2 [30] collisions, have been selected here for comparison and validation of the results provided by the FHO model.

Reaction rates have been determined in the usual way, considering a one-dimensionnal Maxwellian distribution of the particles for averaging of transition probabilities $P(\bar{v})$ [Eqs. (5) and (6)], and multiplying them by the gas-kinetic collision frequency:

Table 1 Data used for the calculation of reaction rates

	α, Å^{-1}	E_m, K	Ref.	σ, Å^2	Ref.
N_2-N_2	4	200	[38]	44	[50]
N_2-N	2.7	18,100	[48]	28	[a]
N_2-O_2	4	200	[38]	40	[b]
O_2-O_2	4	200	[38]	35	[51]

[a]This work [b]Average of N_2-N_2 and O_2-O_2 cross sections

$$k(T) = Z\left(\frac{\tilde{m}}{k_B T}\right)\int_0^{+\infty} P(\bar{v})\exp\left(\frac{-\tilde{m}v^2}{2k_B T}\right)v\,\mathrm{d}v, \quad \text{with} \quad Z = \sigma\sqrt{\frac{8k_B T}{\pi\tilde{m}}} \tag{12}$$

The compiled data used in the determination of the rate coefficients for the different collision pairs (collisional cross sections and Morse intermolecular potentials) are summarized in Table 1.

The comparisons that were carried against the different QCT reaction rates proposed by Billing reproduced very closely the results obtained by Adamovich et al. [23,38]. Here, this comparison is extended by presenting results obtained from the FHO model up to 100,000 K, because such high values may be attained in certain conditions immediately behind the shock wave.

Reaction rate coefficients have been calculated for N_2-N_2 V-T transitions up to 100,000 K, and compared with the QCT rates determined by Billing. Also, to illustrate the inability of FOPT theory for the calculation of reaction rates at high temperatures, FOPT rate coefficients have been determined for the N_2-N_2 V-T transition $20 \rightarrow 19$. The obtained results are displayed in Fig. 2. The gas-kinetic collision rate was also represented to assert if the different models remain below this limit.

As expected, a good agreement is obtained between the predicted rates according to FHO model and the calculations of Billing [29]. This agreement is remarkably good at lower transition quantum numbers (V-T transition $1 \rightarrow 0$). Also, it is verified that reaction rates predicted by the FHO model remain lower than the gas-kinetic rate, even at very high translational temperatures. This allows having a good confidence in the model's predictive capabilities, for a large range of temperatures. It is verified as well that near the high-temperature limit, the reaction rates tend to an asymptotic value. This is a trend that occurs for the generality of the predicted FHO rates at high temperatures. In contrast, although good agreement is verified at lower temperatures, it is verified that the FOPT model predicts rates that quickly start diverging from the FHO rates, roughly above $T = 3000$ K. At higher temperatures, a unphysical situation is even

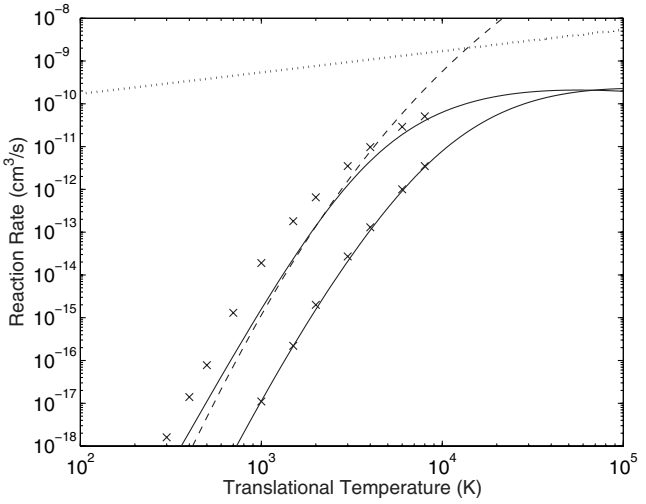

Fig. 2 Single-quantum V-T rates for N_2-N_2: solid line, FHO model; ×, calculations of Billing [29]. V-T transitions $1 \rightarrow 0$ and $20 \rightarrow 19$ displayed from bottom to top. Dashed line, FOPT rate for V-T transition $20 \rightarrow 19$. Dotted line, gas-kinetic collision rate.

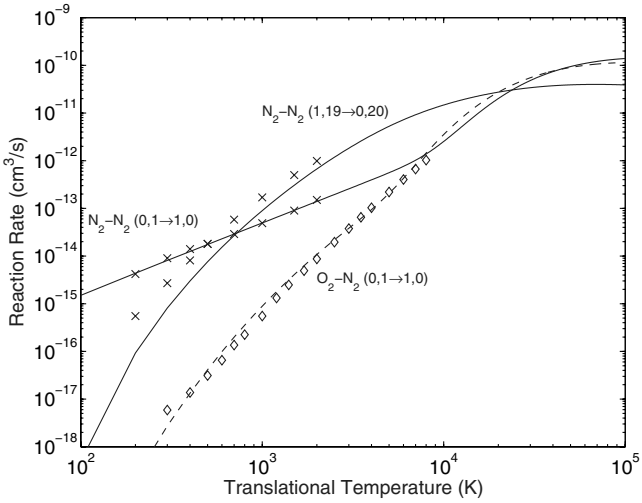

Fig. 3 Single-quantum V-V rates for N_2-N_2 (0, $1 \rightarrow 1$, 0) and (0, $1 \rightarrow 20$, 19) transitions and O_2-N_2 (0, $1 \rightarrow 1$, 0) transitions. Solid and dashed lines, FHO model. ×, calculations of Billing [29] for N_2-N_2. ⋄, interpolation of experimental data for N_2-O_2 (1, $0 \rightarrow 0$, 1) [52].

achieved with the FOPT rates becoming larger than the gas-kinetic rate. This is a well-known consequence of the failure of FOPT theory at larger collision velocities [23]. The calculated transition rates also follow very closely the ones obtained by Adamovich et al. using a purely repulsive potential [23]. This is not surprising as the Morse potential used for the calculation of N_2-N_2 transition probabilities has a very shallow potential well. This implies that the calculated transition probabilities will follow very closely the transitions probabilities obtained using a purely repulsive potential.

Figure 3 presents the comparison between predicted single-quantum, nonresonant V-V rates for different collision pairs. Once again, good agreement is reached between the FHO model and Billing's QCT model for N_2-N_2 collisions, and with the experimental results obtained by Taylor and Bitterman [52] for N_2-O_2 collisions. Interestingly enough, at sufficiently high temperatures, the reaction rates for a given transition become nearly equivalent, independently of the collision partners, if the same intermolecular potential is considered. This is of course a consequence of the vicinity of the molecular masses of N and O. This can also be verified in Fig. 3 for the reaction rates of the V-V transition $(1,\ 0 \rightarrow 0,\ 1)$ when considering N_2-N_2 and N_2-O_2 collisions.

It has been stated by Adamovich et al. [38] that the FHO model cannot successfully predict near-resonant V-V rates at lower

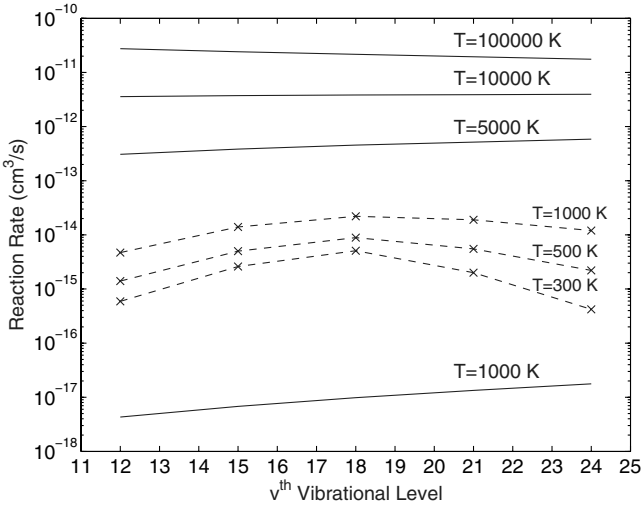

Fig. 4 Near-resonant V-V rates for N_2-O_2 ($v + 1,0 \rightarrow$ v-1,1) transitions. Solid line, FHO model; dashed line with ×, calculations of Billing [31].

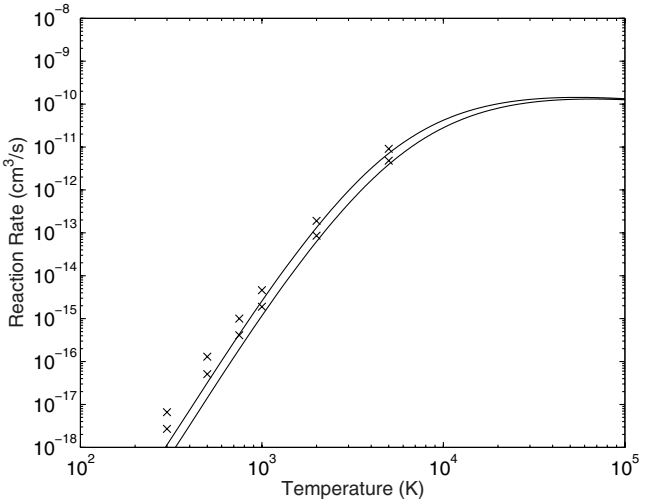

Fig. 5 Single-quantum V-T rates for O_2-O_2. $1 \rightarrow 0$ and $2 \rightarrow 1$ transitions displayed from bottom to top. Solid line, FHO model; ×, calculations of Billing [30].

temperatures, due to the fact that this model considers any transition as a succession of V-T transitions. These act as a bottleneck, compared to the direct resonance transition. This is indeed verified when the predictions of the FHO model are compared with the predictions of Billing's QCT calculations [31] for near-resonant N_2-O_2 V-V transitions. Figure 4 displays the reaction rates predicted by Billing and the ones predicted by the FHO model (the FHO model reaction rates at 300 and 500 K, being several orders of magnitude lower, are not displayed here). It is verified that at higher temperatures (>5000 K), V-T processes become more efficient, eliminating this bottleneck, and the predicted FHO reaction rates become much higher than the lower temperature rates predicted by Billing's model.

Finally a comparison of the FHO model with QCT calculations obtained by Billing [30] is carried out for the prediction of O_2-O_2 V-T rates. This comparison is presented in Fig. 5.

A good agreement is achieved between the two models except at lower temperatures where the reaction rates predicted by the FHO model are slightly lower than those predicted by Billing. This is likely due to the fact that Billing has accounted for quadrupole-quadrupole attractive interactions in the definition of its internuclear potential. These interactions need to be accounted for at lower collision velocities (lower temperatures), which would explain the observed differences in the predicted rates, at temperatures below 1000 K. This is not accounted for in our FHO model, which relies on a simpler Morse intermolecular potential.

III. Application to the Simulation of Postshock Flows

The suitability of the FHO model for the calculation of V-T and V-V-T transition probabilities has been inferred, and a database of rate equations has been developed. It has been chosen to calculate reaction rates at translational temperatures from 100 to 100,000 K through increments of 100 K. The upper limit of 100,000 K has been judged as sufficient to cope with the most extreme atmospheric entry flows. However, these rates can be easily extrapolated to higher temperature values, because they asymptotically tend to a unique value lower than the gas-kinetic collision rate, roughly somewhere from 50,000 to 100,000 K.

A. Challenges and Possible Simplifications for the Application of the FHO Model

For the application of the FHO method to shock-heated flows, a database of reaction rates needs firstly to be built.

An initial issue arises when one has to consider multiquantum transitions. As it will be verified more ahead in this paper, at high translational temperatures typical of a postshock flow (above 10,000 K), reaction rates for multiquantum transitions become of equivalent magnitudes, and transitions between the overall system of quantum states need to be taken into account. Taking only into account the 60 vibrational bound levels of nitrogen, the simulation of all the multiquantum V-T and V-V reaction rates [Eqs. (3) and (4)] results in 60^2 and 60^4 different transitions, respectively. Namely, for the V-V processes, more than 10^7 reaction rates need to be calculated. In practice, the need to calculate such a high number of reaction rates prevents the full simulation of the overall V-T and V-V processes behind a shock wave, to the exception of simpler 1-D geometries. Nevertheless, such simplified geometries still need large computing resources and the application of simplified expressions for the calculation of reaction rates is needed [10].

An additional issue arises for the calculation of transitions between higher vibrational levels. Equations (5) and (6) are poorly conditioned, and the factorial terms cannot be exactly calculated for these higher level transitions. Moreover, it can be easily seen that overflow and underflow situations to the used machine precision will eventually be reached for such transitions. Different approaches may be devised for levelling this issue.

These two issues are discussed in detail in the next sections.

1. *Asymptotic Transition Probabilities*

Expressions of Eqs. (5) and (6) are rather cumbersome. Calculation of the V-T and V-V-T transition probabilities includes a summation of terms which may achieve a broad range of magnitudes near the computational system underflow limit. Indeed, it is easy to recognize that the calculation of V-T transition probabilities between two higher vibrational levels will result in a summation of steadily increasing values from near the underflow limit of the computer system (calculation of the $\exp(-\varepsilon)|\sum_r (-1)^r [r!(i-r)!(f-r)!\,\varepsilon^r]^{-1}|^2$ term). Moreover, this term is to be multiplied to a term near the overflow limit of the computer system (calculation of the $i!f!\varepsilon^{i+f}$ term). Therefore, overflow and underflow exceptions are difficult to avoid, and even so, the multiplication of very large and very small numerical values will result in very poor precision for the obtained results (moreover, the factorial expressions can no longer be calculated exactly for higher numbers). For the expression of V-V-T rates [Eq. (6)], the same comments apply.

Preliminary calculations carried in MATLAB, which provides a 64 bit calculation precision (equivalent to 2.23×10^{-308}–1.80×10^{308} numeric range), showed that for transitions between vibrational quantum numbers typically larger than $v = 20$–40 (depending on the interaction potential), accurate transition probabilities could no longer be calculated (numerical noise, probabilities higher than 1, underflow, and overflow exceptions). Therefore, it is concluded that not even the increased precision of MATLAB (64 bit digits instead of the usual 32–64 bits of languages such as C and FORTRAN) suffices for allowing accurate calculations to be carried out for higher vibrational levels.

Nikitin and Osipov [53] have suggested asymptotical formulas for Eqs. (5) and (6). For such approximations V-T and V-V-T transition probabilities may be rewritten asymptotically as

$$P(i \rightarrow f, \varepsilon) = J_s^2(2\sqrt{n_s \varepsilon}) \tag{13}$$

for $i, f \gg s = |i - f|$, and $n_s = [\max(i, f)!\,\min(i, f)!]^{-s}$, and

$$P(i_1, i_2 \rightarrow f_1, f_2, \varepsilon, \rho) = J_s^2[2(n_s^{(1)} n_s^{(2)} \rho_\xi^2/4)^{1/2}] \tag{14}$$

for $i_1 + i_2 = f_1 + f_2$ and $i_1 + i_2 + f_1 + f_2 \gg s = |i_1 - f_1|$.

In Eqs. (13) and (14) J_s stands for the Bessel function of the first species and sth order.

These expressions prove to be very useful in avoiding underflow and overflow errors in the calculation of V-T and V-V-T transition probabilities, in addition to allowing faster calculation times. However, these asymptotic expressions are unable to fit the initial expressions of Eqs. (5) and (6) at higher collision velocities [53]. A comparison of Eq. (5) and (13) has been carried out for the determination of the V-T transition probability $5 \rightarrow 4$ in a N_2-N_2 collision. Typical Maxwellian energy distribution functions (EDF)

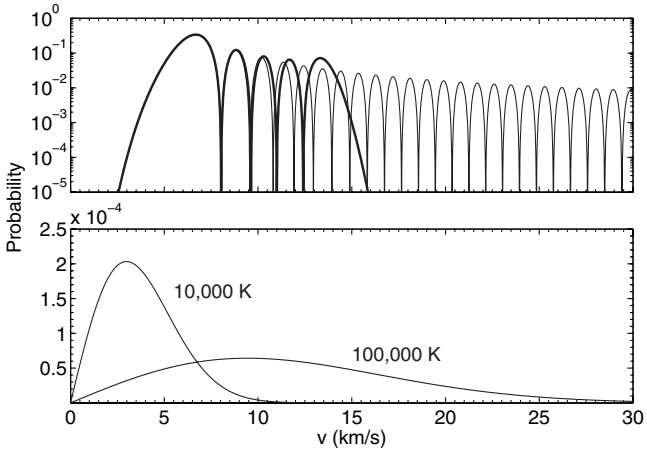

Fig. 6 Exact (bold) and asymptotic probability (light) for a 5 → 4 N_2-N_2 V-T collision (upper figure) and Maxwellian velocity distribution functions at 10,000 and 100,000 K (lower figure).

of N_2 at $T_{tr} = 10,000$ and 100,000 K have also been determined. The obtained results are presented in Fig. 6 against the colliding velocity.

It can be observed that for higher collision velocities (typically $v > 10$ km/s), the asymptotic expression proposed by Nikitin and Osipov is no longer valid. Interestingly enough, it is verified that the integration of both expressions with maxwellian EDF's give very similar predicted reaction rates, independently of the temperature range. For lower translational temperatures ($\leq 10,000$ K), the EDF mainly overlaps the part where both models allow very close values. Although not valid at higher collision velocities, the transition probability predicted by Nikitin and Osipov's expression has an equivalent area to the exact expression, and this results in similar predicted rates. Therefore, for practical purposes, Nikitin and Osipov's expressions can be used without a sensible loss of accuracy.

Additional simplifications for Nikitin and Osipov's transition probabilities have been proposed by Adamovich et al. [23,38]

$$J_s^2(2\sqrt{n_s\varepsilon}) \cong \frac{(n_s)^s}{(s!)^2}\varepsilon^s \exp\left(\frac{-2n_s\varepsilon}{s+1}\right) \tag{15}$$

$$J_s^2\left[2\left(n_s^{(1)}n_s^{(2)}\rho_\xi^2/4\right)^{1/2}\right] \cong \frac{\left[n_s^{(1)}n_s^{(2)}\right]^s}{(s!)^2}\left(\frac{\rho_\xi^2}{4}\right)^s \exp\left(-\frac{n_s^{(1)}n_s^{(2)}}{s+1}\frac{\rho_\xi^2}{4}\right) \tag{16}$$

These approximations work well for transitions involving small quanta exchange. However, for larger quantum number transitions, such expressions become unreliable, and the predicted transition probabilities may even exceed unity, with important consequences in the calculation of reaction rates at higher temperatures. An example is presented in Fig. 7 for a 15 → 30 N_2-N_2 V-T collision.

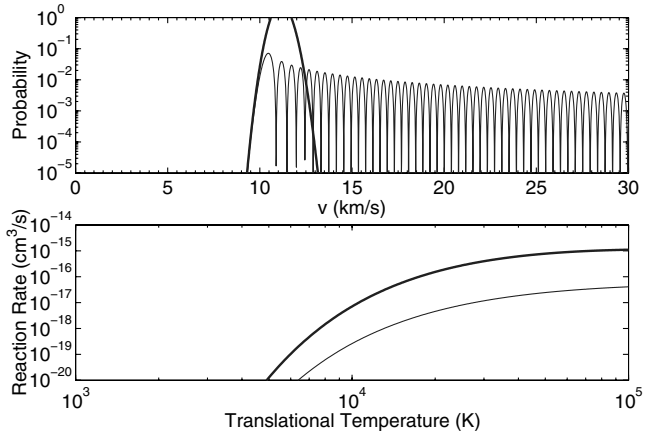

Fig. 7 Nikitin (light) and Adamovich (bold) asymptotic transition probabilities for a 15 → 30 N_2-N_2 V-T collision as a function of the colliding velocity (upper figure) and corresponding reaction rates against the translational temperature (lower figure).

In short, the motivations of our work being related to the simulation of postshock flows at hyperbolic velocities, such asymptotic expressions cannot be applied, as they would result in different predicted rate coefficients for the temperature range 10,000–100,000 K. Instead, a greater accuracy is retained here when using Eqs. (5) and (6) for the calculation of V-T and V-V-T probabilities.

For this work, it has been chosen to devise a method allowing the numerical implementation of the exact transition probabilities [Eqs. (5) and (6)]. The problem has been solved by using the symbolic math toolbox included in MATLAB for an exact calculation of the factorial factors in Eqs. (5) and (6), and the calculation of the other parameters of the equations using variable precision arithmetics. An accuracy of 32–64 digits has allowed one to obtain rate coefficients for transitions between any vibrational level up to $v = 100$. This solution comes at a cost of larger calculation times (typically 30 min on a Pentium 4 at 3 GHz for transitions between the higher vibrational levels). Owing to the extremely larger computational overhead, transition probabilities where calculated using standard MATLAB with 64 bit numerical precision for transitions between lower vibrational levels, and completed with variable precision arithmetics for transitions where 64 bit arithmetics fail in providing accurate results.

2. *Reduction of the Number of Calculated Rates*

At very high translational energies with $E_{tr} \gg E_{vib}$, such as behind a strong shock wave, it has been verified that V-V-T processes occur as two independent V-T processes such that the corresponding probability is given by [37,38]

$$P(i_1, i_2 \to f_1, f_2, \varepsilon, \rho) \cong P(i_1 \to f_1, \varepsilon)P(i_2 \to f_2, \varepsilon) \tag{17}$$

Purely V-V exchange processes can therefore be neglected in this case and summing over all of the possible vibrational states of the *CD* molecule can be performed. This hypothesis holds approximately for $T \geq 10,000$ K [23]. The FHO transition probability scaling is then equivalent to the expression of Eq. (5) for molecule atom collisions

$$P(i_1, \text{all} \to f_1, \text{all}, \varepsilon, \rho) = P(i_1 \to f_1, \varepsilon) \tag{18}$$

B. Modeling of Dissociation Processes

State-specific dissociation rates according to the process

$$AB(i) + M \rightleftarrows A + B + M \tag{19}$$

may be determined using the FHO method, according to the approach proposed and discussed by Macheret and Adamovich [40]. The probability for dissociation can be calculated as the product of the transition probability to a quasi-bound[‖] state such that $v > n$, with $n = 59$ denoting the last bound vibrational level, times the probability of the subsequent decay of the energetic complex

$$P(i \to, \varepsilon) = P(i \to v_{\text{qbound}}, \varepsilon)P_{\text{decay}} \tag{20}$$

with $P_{\text{decay}} \sim 1$. This assumption is not entirely justified when v is much higher than n, the formation of an intermediary quasi-bound state being unlikely . However, for dissociation processes behind a shock wave with $E_{tr} \gg E_{vib}$, occurring directly from the lower vibrational levels, this assumption provides a realistic approximation to the gas dissociation rates.

[‖]The concept of a quasi-bound state must be understood here as a vibrational level above the dissociation limit, solely bound by the repulsive part of the intramolecular potential.

IV. Simulation of Dissociation Processes in High-Energy Nitrogen Shock Waves

The FHO model has been applied to the simplified simulation of N_2 dissociation processes behind high-energy shock waves. Nitrogen is the major constituent of Earth's atmosphere, and therefore the analysis of such dissociation processes has a clear relevance for the prediction of high-speed hyperbolic entry flows in Earth.

A. Development of a Complete Database of Nitrogen V-T and Dissociation Rates up to 100,000 K

A database of reaction rates has therefore been previously developed for V-T and V-V-T transitions in N_2 molecules. It is now necessary to determine how many quasi-bound states need to be considered for the simulation of high-temperature postshock flows. The more restrictive case obviously happens for the maximal temperature of 100,000 K considered in our study. Here, a large amount of translational energy is available, which allows that transitions with large quantum jumps may occur. A preliminary analysis of the different predicted reaction rates at 100,000 K has showed that a maximum vibrational level $v = 100$ needs to be considered. Selecting a lesser number of vibrational levels would have a nonnegligible impact on the overall dissociation processes behind the shock wave, as transitions which may still considerably populate such higher levels would be neglected. On the other hand, reaction rates populating vibrational levels with $v > 100$ decrease exponentially, even in the high-temperature limit, and therefore such levels can be safely disregarded in our model.

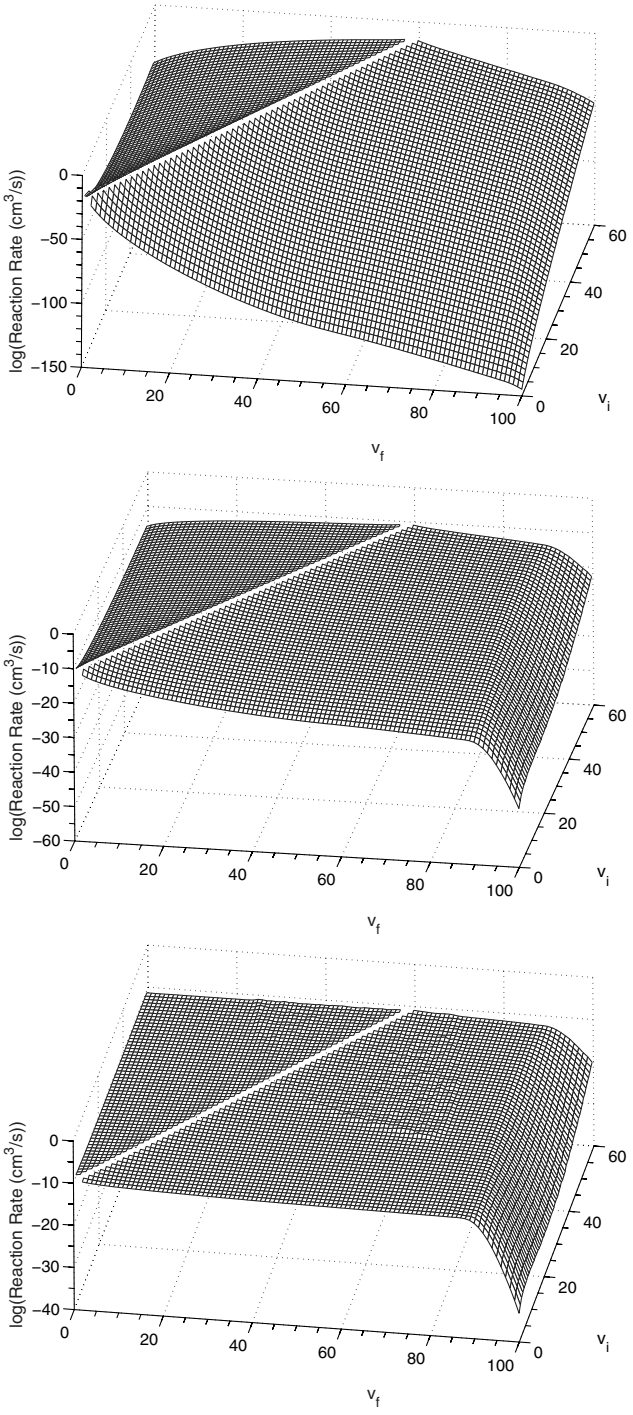

Fig. 8 V-T reaction rates at 1000, 10,000, and 100,000 K, from top to bottom.

According to Sec. II, a full set of V-T rates has been determined using Eq. (18) for 100 levels of N_2. This results in a 61×101 matrix in a 100–100,000 K temperature range (transitions between quasi-bound levels $v = 59$–100 are disregarded as dissociation of the molecule is considered to occur after a transition to a quasi-bound level). The predicted rates at 1000, 10,000, and 100,000 K are presented in Fig. 8.

An analysis of the matrix of rate coefficients at lower temperatures (1000 K) shows a sharp decrease for multiquantum transitions, especially in the case of transitions from lower to upper levels. This a well-known trend, because at lower temperatures multiquantum transitions may be safely disregarded in a state-to-state model. However, for rate coefficients at higher temperatures, outside the domain of application of usual state-to-state models ($>10,000$ K), it is verified that multiquantum transition rates become increasingly important, and at the high-temperature limit for this study (100,000 K), a plateau is reached because transitions between any vibrational level of N_2 become equiprobable.

This last point has a major relevance for the simulation of atmospheric entry flows, implying that the full matrix set of reaction rates between any level of N_2 needs to be taken into account, instead of considering solely single-quantum transitions as it is usual in aerospace applications [54]. Unfortunately, this implies considering a much larger reaction rate set in the simulation of entry flows, which may be computationally unfeasible at the time.

Finally, an abrupt decrease of the reaction rates populating the vibrational levels $v > 90$ is observed, which validates our assumption of considering a maximum quasibound level v equal to 100 in our FHO model. Interestingly enough, the use of polynomial expansions [Eq. (11)] for the calculation of vibrational level energies, instead of the more accurate RKR method, would have prevented the calculation of level energies for $v > 81$, as the application of Eq. (11) using the usual spectroscopic constants of N_2 results in an artificial plateau at $v = 81$. Furthermore, Eq. (11) also provides erroneous values for the level energies from sensibly $v = 40$ [42]. This restriction has prevented higher quasi-bound levels to be considered in other works using the FHO model [40]. Moreover, the accuracy of the calculated reaction rates for energy levels above $v = 40$ becomes questionable, as it depends on poorly predicted energies.

B. Simulation of State-Resolved Dissociation Processes Behind a Strong Shock Wave

To evaluate the dissociation channels behind a shock wave, the developed reaction rates sets have been applied to the simulation of simplified shock geometries. Here, a gas at an initial equilibrium temperature of $T = 195$ K and at a density corresponding to an altitude of 76 km (conditions typical of an atmospheric entry [55]) is heated by a shock wave to a translational temperature of 1000, 10,000, and 100,000 K. Relaxation of the translational temperature is disregarded behind the shock, which means that the translational mode of the nitrogen molecules acts as an infinite energy reservoir, with different energy transfer rates (which depend on the translational temperature). This limiting case is useful for evaluating the behavior of the different V-T processes at different temperatures retaining temperature specific reaction rates (see Fig. 8). Also, to

limit the scope of the study to the analysis of the dissociation channels behind a shock wave, recombination processes are disregarded. We note that these will only be important at lower temperatures. State-resolved vibrational kinetics are simulated here, according to the usual system of master equations [10], and using the aforementioned rate coefficient database.

The obtained time-dependent vibrational distribution functions (VDF) are presented in Fig. 9 for three translational temperatures (once more 1000, 10,000, and 100,000 K). The populations of the quasi-bound levels ($v = 59$–100) are also presented to evaluate their importance in the overall dissociation rate (here we are considering that the population of such levels corresponds in practice to the dissociation of the molecule). At 1000 K, the translational temperature is too low to induce noticeable dissociation of the flow molecules, and the VDF tends to an equilibrium Boltzmann distribution. At 10,000 K, the temperature is sufficiently high to allow the establishment of dissociation reactions. The higher levels are progressively populated (without the occurrence of a plateau in the population of the intermediary levels) until dissociation is progressively established, ultimately leading to the depopulation of the overall bound levels (for $t > 10^{-2}$ s). It is verified that dissociation occurs primarily from the first quasi-bound levels close to the dissociation limit, with a sharp decrease of dissociation processes from quasi-bound levels with $v > 90$. In the most severe dissociation case at 100,000 K, population of the overall vibrational levels occurs equiprobably, as expected according to the examination of the reaction rates presented in Fig. 8. A plateau in the population of the different vibrational levels is observed up to $v = 90$ where the population of the upper levels also abruptly decreases, similarly to the case where $T = 10,000$ K. Dissociation of the overall molecules proceeds very quickly in this limiting case (the flow is completely dissociated at $t = 10^{-5}$ s).

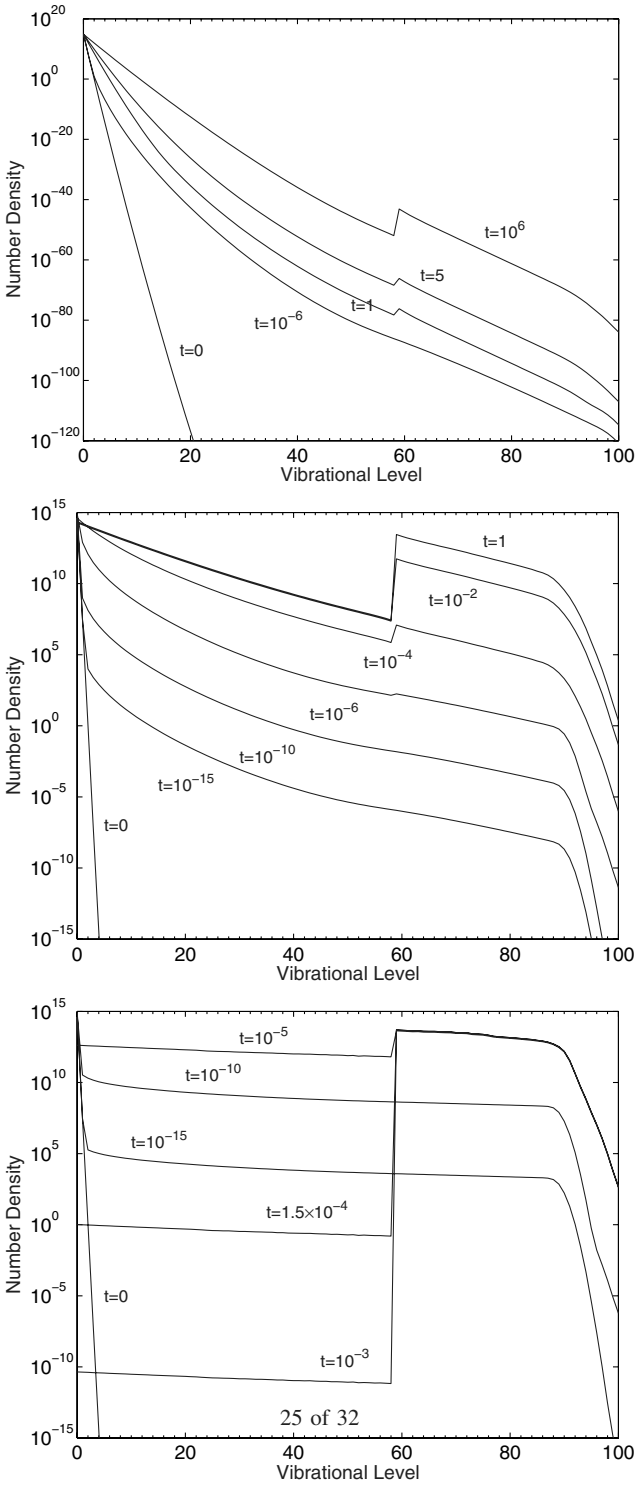

Fig. 9 Time evolution of postshock N_2 VDFs (T_{tr} = 1000, 10,000, and 100,000 K from top to the bottom).

Finally, the time evolution of the fractional molecular dissociation is displayed in Fig. 10, for different shock temperatures.

At higher translational temperatures ($T > 50,000$ K), the time increase of the dissociated fraction of the flow exhibits a constant slope, which confirms that dissociation occurs equiprobably from any vibrational level of the N_2 molecule. At lower temperatures ($T < 25,000$ K), a sharp increase in the dissociated fractions is observed, which indicates the existence of a ladder-climbing phenomenon only noticeable at lower temperatures. This is typically the phenomenon that contributes for dissociation in other lower-temperature applications such as gas discharges [21], where only single-quantum transitions are considered. Also the determinant influence of the shock temperature on the delay after which the flow is completely dissociated is clearly seen. At 100,000 K the flow is completely dissociated after roughly 1 μs, at 10,000 K the flow is completely dissociated after 1 s, and at shock temperatures roughly below 7000 K larger times are required to achieve complete dissociation.

C. Thermal Dissociation Rates Predicted by the FHO Model

A further validation of the FHO model has been carried through a comparison with thermal dissociation rates proposed by different authors. In previous works, Adamovich and Macheret have extended the FHO model to include three-dimensional and rotation effects for atom-diatom V-T processes [39], and for diatom-diatom V-T and V-V processes at moderate collision velocities [41]. Thermal dissociation rates have been obtained by the authors [40] and compared to a good agreement with experimentally-determined dissociation rates for N_2-N_2 collisions. Here, we have further

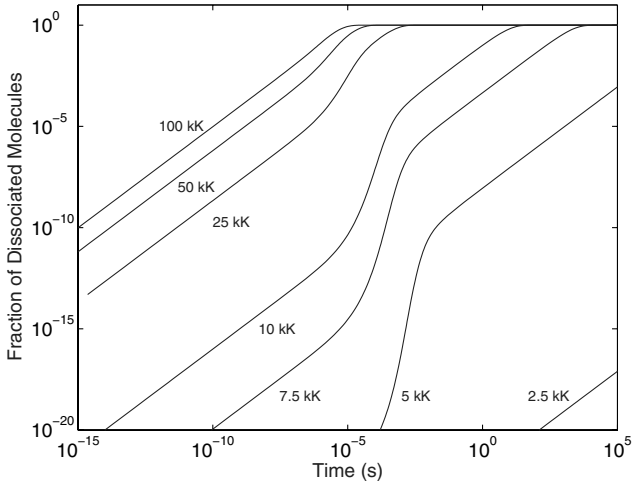

Fig. 10 Time evolution of N_2 dissociation at different shock temperatures.

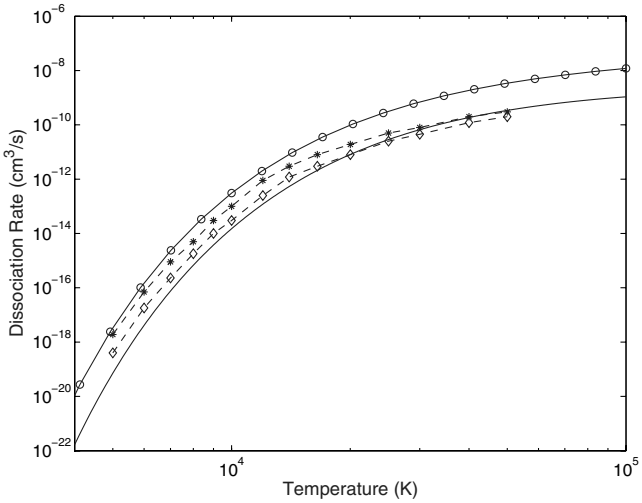

Fig. 11 Thermal dissociation rates of nitrogen from N_2-N_2 collisions. Solid line, FHO model (this work); dashed line with +, 3-D FHO model, impulsive approach [40]; dashed line with ⋄, 3-D FHO model, free-rotation approach [40]; dashed line with ∘; experimental rate [56].

compared the thermal dissociation rates predicted by our FHO model with such previously determined rates, as well as with experimental dissociation rates proposed by Shatalov [56]. Such dissociation rates are compared in Fig. 11.

Overall, it is verified that a good agreement is found between the dissociation rates predicted by the different models using the FHO approach. The agreement with the experimentally determined dissociation rate is also adequate, although the rates predicted by the FHO models fall below this dissociation rate by 1–2 orders of magnitude. Comparing the rates predicted by the authors' 1-D FHO model with the rates predicted by the 3-D model of Adamovich and Macheret, explicitly accounting for 3-D and rotational effects, results in about an order of magnitude increase of the predicted rates. However, at higher temperatures, the dissociation rates predicted by the 1-D model increase more sharply than the dissociation rates predicted by the 3-D model. This is likely to result from the improved RKR calculation of the vibrational levels energies, as applied in our model. Accounting for 60 instead of 46 bound vibrational levels, as well as considering a maximum vibrational level $v_{\max} = 100$ instead of $v_{\max} = 81$ has been verified to increase the dissociation rates by at least 1 order of magnitude.

V. Concluding Remarks

The forced harmonic oscillator theory has been shown to be adequate for the description of shock-induced dissociation processes during an atmospheric entry. Once the practical difficulties associated with the numerical calculation of transition probabilities are coped with using appropriate methods, the method can be used to yield an adequate and complete set of rate coefficients valid up to very high temperatures. The agreement between the state-resolved rates predicted by our model and other state-resolved rates is excellent. The dissociation rates predicted by our model achieve an adequate agreement with experimentally determined rates although the former fall 1–2 orders of magnitude lower.

One improvement that can be considered as having been brought by the application of the forced harmonic oscillator theory for the simulation of atmospheric entry shock waves is the availability of reaction rates up to very high temperatures. Obviously, the obtained rates can only be considered as tentative as the considered high-temperature range is beyond the common limits of experimental validations and other dynamic calculations. However, the adequate agreement of the predicted rates at lower temperatures, as well as the physical adequacy of the reaction rates at high temperatures (which remain well below the kinetic collision rate), allows having confidence of the adequacy of this model for a tentative prediction of very high-temperature state-resolved reaction rates.

Furthermore it has been shown that at such higher temperatures, the collisional processes differ greatly from those seldom encountered at lower temperatures. It has been verified that multiquantum transitions become preponderant, and need to be taken into account if one is to accurately simulate high-temperature dissociation processes. Also, it has been verified that uncertainties on the determination of the higher-lying vibrational levels energies sensibly affect the quality of the predicted reaction rates. The Rydberg–Klein–Rees method, which has been used in this work, can be considered as a first improvement towards the determination of the higher vibrational levels close to the dissociation limit. Using other accurate approaches could also bring some further insights on this question.

In brief, the approach presented in this paper is a first step towards the development of a full collisional-radiative model for the simulation of high-speed atmospheric entries. The state-resolved rates presented in this work can be considered as a tentative but solid basis where more elaborate descriptions can be developed, for example, explicitly taking into account rotational effects, or interactions between different molecular electronic levels.

Acknowledgments

The authors would like to thank I. V. Adamovich for fruitful discussions about the FHO model, and for sending the source codes of his own FHO model, which were used for comparison purposes.

References

[1] Koffi-Kpante, K., Zeitoun, D., and Labracherie, L., "Computation and Experimental Validation of N_2-CH_4 Mixture Flows Behind Normal Shock Wave," *Shock Waves* Vol. 7, No. 6, 1997, pp. 351–361.

[2] Gorelov, V. A., Gladyshev, M. K., Kireev, A. Y., Yegorov, I. V., Plastinin, Y. A., and Karabadzhak, G. F., "Experimental and Numerical Study of Nonequilibrium Ultraviolet NO and N_2^+ Emission in Shock Layer," *Journal of Thermophysics and Heat Transfer*, Vol. 12, No. 2, 1998, pp. 379–388.

[3] Abe, K., Kihara, H., Uchida, T., and Nishida, M., "Experimental and Numerical Studies of Rotational Relaxation Behind a Strong Shock Wave in Air," *Shock Waves*, Vol. 11, No. 6, 2002, pp. 413–421.

[4] Losev, S. A., Pogosbekian, M. Y., Sergievskaya, A. L., Kustova, E. V., and Nagnibeda, E. A., "State-to-State Reaction Rate Coefficients, Distributions and Gas Dynamics Behind Strong Shock Waves," *Rarefied Gas Dynamics*, edited by M. Capitelli, Vol. 762, American Institute of Physics, AIP Conference Proceedings, Melville, New York, 2004, pp. 1049–1054.

[5] Anderson, J. D., *Hypersonic and High Temperature Gas Dynamics*, AIAA General Publication Series, AIAA, Reston, VA, 2000.

[6] Capitelli, M., Ferreira, C. M., Gordiets, B. F., and Osipov, A. I., *Plasma Kinetics in Atmospheric Gases*, Springer Series on Atomic, Optical and Plasma Physics, Springer, Heidelberg, Germany, 2000.

[7] Kewley, D. J., "Numerical Study of Anharmonic Diatomic Relaxation Rates in Shock Waves and Nozzles," *Journal of Physics B: Atomic and Molecular Physics*, Vol. 8, No. 15, 1975, pp. 2565–2579.

[8] Lordet, F., Méolans, J. G., Chauvin, A., and Brun, R., "Nonequilibrium Vibration-Dissociation Phenomena Behind a Propagating Shock Wave: Vibrational Population Calculation," *Shock Waves*, Vol. 4, No. 6, 1995, pp. 299–312.

[9] Josyula, E., Basey, W. F., and Ruffin, S. M., "Reactive and Nonreactive Vibrational Energy Exchanges in Nonequilibrium Hypersonic Flows," *Physics of Fluids*, Vol. 15, No. 10, 2003, pp. 3223–3235.

[10] Adamovich, I. V., Macheret, S. O., Rich, J. W., and Treanor, C. E., "Vibrational Relaxation and Dissociation Behind Shock Waves Part 2: Master Equation Modeling," *AIAA Journal*, Vol. 33, No. 6, 1995, pp. 1070–1075.

[11] Capitelli, M., Colonna, G., and Esposito, F., "On the Coupling of Vibrational Relaxation with the Dissociation-Recombination Kinetics: From Dynamics to Aerospace Applications," *Journal of Physical Chemistry A*, Vol. 108, No. 41, 2004, pp. 8930–8934.

[12] Schwartz, R. N., Slawsky, Z. I., and Herzfeld, K. F., "Calculation of Vibrational Relaxation Times in Gases," *Journal of Chemical Physics*, Vol. 20, No. 10, 1952, pp. 1591–1599.

[13] Herzfeld, K. F., and Litovitz, T. A., *Absorption and Dispersion of Ultrasonic Waves*, Academic Press, New York, 1959, Chap. 3.

[14] Rapp, D., and Sharp, T. E., "Vibrational Energy Transfer in Molecular Collisions Involving Large Transition Probabilities," *Journal of Chemical Physics*, Vol. 38, No. 11, 1963, pp. 2641–2648.

[15] Rapp, D., and Englander-Golden, P., "Resonant and Near-Resonant Vibrational-Vibrational Energy Transfer Between Molecules in Collisions," *Journal of Chemical Physics*, Vol. 40, No. 2, 1964, pp. 573–575.
[16] Rapp, D., and Englander-Golden, P., "Erratum: Resonant and Near-Resonant Vibrational-Vibrational Energy Transfer Between Molecules in Collisions," *Journal of Chemical Physics*, Vol. 40, No. 10, 1964, pp. 3120–3121.
[17] Rapp, D., "Interchange of Vibrational Energy Between Molecules in Collisions," *Journal of Chemical Physics*, Vol. 43, No. 1, 1965, pp. 316–317.
[18] Rapp, D., and Kassal, T., "The Theory of Vibrational Energy Transfer Between Simple Molecules in Nonreactive Collisions," *Chemical Reviews (Washington, DC)*, Vol. 69, No. 1, 1969, pp. 61–102.
[19] Cotrell, T. L., and Ream, N., "Transition Probability in Molecular Encounters Part 1. The Evaluation of Perturbation Integrals," *Transactions of the Faraday Society*, Vol. 51, No. 1, 1955, pp. 159–171.
[20] Sharma, R. D., and Brau, C. A., "Energy Transfer in Near-Resonant Molecular Collisions Due to Long-Range Forces With Application to Transfer of Vibrational Energy from ν_3 Mode of CO_2 to N_2," *Journal of Chemical Physics*, Vol. 50, No. 2, 1969, pp. 924–930.
[21] Guerra, V., and Loureiro, J., "Non-Equilibrium Coupled Kinetics in Stationary N_2-O_2 Discharges," *Journal of Physics D: Applied Physics*, Vol. 28, No. 9, 1995, pp. 1903–1918.
[22] Billing, G. D., "Vibration-Vibration and Vibration-Translation Energy Transfer, Including Multiquantum Transitions in Atom-Diatom and Diatom-Diatom Collisions," *Nonequilibrium Vibrational Kinetics*, Springer–Verlag, Berlin, 1986, Chap. 4, pp. 85–111.
[23] Adamovich, I. V., Macheret, S. O., Rich, J. W., and Treanor, C. E., "Vibrational Relaxation and Dissociation Behind Shock Waves Part 1: Kinetic Rate Models," *AIAA Journal*, Vol. 33, No. 6, 1995, pp. 1064–1069.
[24] Secrest, D., "Vibrational Excitation 1: The Quantal Treatment," *Atom-Molecule Collision Theory*, Plenum, New York, 1979, Chap. 11, pp. 377–390.
[25] Secrest, D., and Johnson, B. R., "Exact Quantum Mechanical Calculations of a Mechanical Collinear Collision of a Particle With a Harmonic Oscillator," *Journal of Chemical Physics*, Vol. 45, No. 12, 1966, pp. 4556–4570.
[26] Chapuisat, X., Bergeron, G., and Launay, J.-M., "A Quantum-Mechanical Collinear Model Study of the Collision N_2-O_2," *Chemical Physics*, Vol. 20, No. 2, 1977, pp. 285–298.
[27] Chapuisat, X., and Bergeron, G., "Anharmonicity Effects in the Collinear Collision of Two Diatomic Molecules," *Chemical Physics*, Vol. 36, No. 3, 1979, pp. 397–405.
[28] Billing, G. D., and Fisher, E. R., "VV and VT Rate Coefficients in H_2 by a Quantum-Classical Model," *Chemical Physics*, Vol. 18, Nos. 1–2, 1976, pp. 225–232.
[29] Billing, G. D., and Fisher, E. R., "VV and VT Rate Coefficients in N_2 by a Quantum-Classical Model," *Chemical Physics*, Vol. 43, No. 3, 1979, pp. 395–401.
[30] Billing, G. D., and Kolesnick, R. E., "Vibrational Relaxation of Oxygen. State-to-State Rate Constants," *Chemical Physics Letters*, Vol. 200, No. 4, 1992, pp. 382–386.
[31] Billing, G. D., "VV and VT Rates in N_2-O_2 Collisions," *Chemical Physics*, Vol. 179, No. 3, 1994, pp. 463–467.
[32] Billing, G. D., "Vibrational/Vibrational Energy Transfer in CO Colliding With $^{14}N_2$, $^{14}N^{15}N$ and $^{15}N_2$," *Chemical Physics*, Vol. 50, No. 2, 1980, pp. 165–173.
[33] Cacciatore, M., and Billing, G. D., "Semiclassical Calculations of VV and VT Rate Coefficients in CO," *Chemical Physics*, Vol. 58, No. 3, 1981, pp. 395–407.
[34] Kerner, E. H., "Note on the Forced and Damped Oscillations in Quantum Mechanics," *Canadian Journal of Physics*, Vol. 36, No. 3, 1958, pp. 371–377.
[35] Treanor, C. E., "Vibrational Energy Transfer in High-Energy Collisions," *Journal of Chemical Physics*, Vol. 43, No. 2, 1965, pp. 532–538.
[36] Zelechow, A., Rapp, D., and Sharp, T. E., "Vibrational-Vibrational-Translational Energy Transfer Between Two Diatomic Molecules," *Journal of Chemical Physics*, Vol. 49, No. 1, 1968, pp. 286–299.
[37] Adamovich, I. V., Rich, J. W., and Macheret, S. O., "Existence of a Bottleneck in Vibrational Relaxation of Diatomic Molecules," *Journal of Thermophysics and Heat Transfer*, Vol. 11, No. 2, 1997, pp. 261–265.
[38] Adamovich, I. V., Macheret, S. O., Rich, J. W., and Treanor, C. E., "Vibrational Energy Transfer Rates Using a Forced Harmonic Oscillator Model," *Journal of Thermophysics and Heat Transfer*, Vol. 12, No. 1, 1998, pp. 57–65.
[39] Adamovich, I. V., and Rich, J. W., "Three-Dimensional Nonperturbative Analytic Model of Vibrationally Energy Transfer in Atom-Molecule Collisions," *Journal of Chemical Physics*, Vol. 109, No. 18, 1998, pp. 7711–7724.
[40] Macheret, S. O., and Adamovich, I. V., "Semiclassical Modeling of State-Specific Dissociation Rates in Diatomic Gases," *Journal of Chemical Physics*, Vol. 113, No. 17, 2000, pp. 7351–7361.
[41] Adamovich, I. V., "Three-Dimensional Analytic Model of Vibrational Energy Transfer in Molecule-Molecule Transitions," *AIAA Journal*, Vol. 39, No. 10, 2001, pp. 1916–1925.
[42] Lino da Silva, M., and Dudeck, M., "Arrays of Radiative Transition Probabilities for CO_2-N_2 Plasmas," *Journal of Quantitative Spectroscopy and Radiative Transfer*, (to be published).
[43] Deleon, R., and Rich, J. W., "Vibrational Energy Exchange Rates in Carbon Monoxide," *Chemical Physics*, Vol. 107, No. 2, 1986, pp. 283–292.
[44] Yang, X., Kim, E. H., and Wodtke, A. M., "Vibrational Energy Transfer of Very Highly Vibrationally Excited NO," *Journal of Chemical Physics*, Vol. 96, No. 7, 1992, pp. 5111–5122.
[45] Price, J. M., Mack, J. A., Rogaski, C. A., and Wodtke, A. M., "Vibrational-State-Specific Self-Relaxation Rate Constant Measurements of Highly Excited $O_2(v = 19–28)$," *Chemical Physics*, Vol. 175, No. 1, 1993, pp. 83–98.
[46] Park, H., and Slanger, T. G., "$O_2(X, v = 8–22)$ 300 K Quenching Rate Coefficients for O_2 and N_2, and $O_2(X)$ Vibrational Distribution From 248 nm O_3 Photodissociation," *Journal of Chemical Physics*, Vol. 100, No. 1, 1994, pp. 287–300.
[47] Klatt, M., Smith, I. W. M., Tuckett, R. P., and Ward, G. N., "State-Specific Rate Constants for the Relaxation of $O_2(X^3\Sigma_g^-)$ from Vibrational Levels $v = 8$ to 11 by Collisions With NO_2 and O_2," *Chemical Physics Letters*, Vol. 224, No. 3/4, 1994, pp. 253–257.
[48] Lagana, A., Garcia, E., and Ciccarelli, L., "Deactivation of Vibrationally Excited Nitrogen Molecules by Collision with Nitrogen Atoms," *Journal of Physical Chemistry*, Vol. 91, No. 2, 1987, pp. 312–314.
[49] Lagana, A., and Garcia, E., "Temperature Dependence of $N + N_2$ Rate Coefficients," *Journal of Physical Chemistry*, Vol. 98, 1994, No. 2, pp. 502–507.
[50] Hirschfelder, J. O., Curtiss, C. F., and Bird, R. B., *Molecular Theory of Gases and Liquids*, John Wiley, New York, 1954.
[51] Kiefer, J. H., "Effect of VV Transfer on the Rate of Diatomic Dissociation," *Journal of Chemical Physics*, Vol. 57, No. 5, 1972, pp. 1938–1956.
[52] Taylor, R. L., and Bitterman, S., "Survey of Vibrational Relaxation Data for Processes Important in the CO_2-N_2 Laser System," *Reviews of Modern Physics*, Vol. 41, No. 1, 1969, pp. 26–47.
[53] Nikitin, E. E., and Osipov, A. I., "Vibrational Relaxation in Gases," *Kinetic and Catalysis*, Vol. 4, VINITI, All-Union Institute of Scientific and Technical Information, Moscow, 1977, Chap. 2.
[54] Capitelli, M., Armenise, I., and Gorse, C., "State-to-State Approach in the Kinetics of Air Components Under Re-Entry Conditions," *Journal of Thermophysics and Heat Transfer*, Vol. 11, No. 4, 1997, pp. 570–578.
[55] Hartung, L. C., "Hypersonic, Nonequilibrium Flow over the FIRE II Forebody at 1634 sec," NASA TM 109141, 1994.
[56] Shatalov, O. P., "Recommended Data on Rate Constants of Physical and Chemical Processes in N-O Atoms System," Moscow State University—Russia, Institut of Mechanics AVOGADRO Center, Moscow, 1990.